Available online at www.sciencedirect.com
ScienceDirect
Energy Conversion and Management 48 (2007) 2925–2933
ENERGY CONVERSION & MANAGEMENT
www.elsevier.com/locate/enconman

Cylinder wall insulation effects on the first- and second-law balances of a turbocharged diesel engine operating under transient load conditions

E.G. Giakoumis *

Internal Combustion Engines Laboratory, Thermal Engineering Department, School of Mechanical Engineering, National Technical University of Athens, 9 Heroon Polytechniou Street, Zografou Campus, 15780 Athens, Greece

Available online 27 August 2007

Abstract

During the last decades there has been an increasing interest in the low heat rejection (LHR) diesel engine. In an LHR engine, an increased level of temperatures inside the cylinder is achieved, resulting from the insulation applied to the walls. The steady-state, LHR engine operation has been studied so far by applying either first- or second-law balances. Only a few works, however, have treated this subject during the very important transient operation with the results limited to the engine speed response. To this aim an experimentally validated transient diesel engine simulation code has been expanded so as to include the second-law balance. Two common insulators for the engine in hand, i.e. silicon nitride and plasma spray zirconia are studied and their effect is compared to the nominal non-insulated operation from the first- and second-law perspective. It is revealed that after a step increase in load, the second-law values unlike the first-law ones are heavily impacted by the insulation scheme applied. Combustion and total engine irreversibilities decrease significantly (up to 23% for the cases examined) with increasing insulation. Unfortunately, this decrease is not transformed into an increase in the mechanical work but rather increases the potential for extra work recovery owing to the higher availability content of the exhaust gas.

Keywords: Turbocharged diesel engine; Transient operation; Second-law; Exergy; Irreversibilities; Insulation

1. Introduction

The turbocharged compression ignition (diesel) engine is nowadays the most preferred prime mover in medium and medium-large units applications (truck driving, land traction, ship propulsion, electrical generation), owing to its reliability that is combined with excellent fuel efficiency. However, its transient operation is often linked with off-design (e.g. turbocharger lag) and consequently non-optimum performance. This often leads to unacceptable exhaust emissions and poor speed response, and on the other hand, points out the significance of proper interconnection between the various engine components (governor, fuel pump, turbocharger and load).

During the last decades, diesel engine modelling and experimental investigation has helped enormously as regards the study and optimisation of transient operation. Several works have been published that deal with fundamental or parametric studies of transient response (e.g. [1–4]). On the other hand, it has long been understood that traditional first-law analysis, which is needed for modelling the engine processes, often fails to give the engineer the best insight into the engine's operation. In order to analyse engine performance – that is, evaluate the inefficiencies associated with the various processes – second-law analysis must be applied [5,6]. For second-law analysis, the key concept is "availability" (or exergy). The availability content of a material represents its potential to do useful work. Unlike energy, availability can be destroyed which is a result of such phenomena as combustion, friction, mixing or throttling. The destruction of availability – usually

* Tel.: +30 210 772 1360; fax: +30 210 772 1343.
E-mail address: vgiakms@central.ntua.gr

0196-8904/$ - see front matter © 2007 Elsevier Ltd. All rights reserved.
doi:10.1016/j.enconman.2007.07.013

Nomenclature

A	availability (exergy) (J)
b	flow availability (flow exergy) (J/kg)
D	cylinder bore (m)
F	surface area (m^2)
h	specific enthalpy (J/kg) or heat transfer coefficient (W/m^2 K)
I	irreversibilities (J)
k	thermal conductivity (W/m K)
N	engine speed (rpm)
p	pressure (bar)
Q	heat (J)
s	specific entropy (J/kg K)
T	temperature (K)
t	time (s)
V	volume (m^3)

Greek letters

α	thermal diffusivity (m^2/s)
μ	chemical potential (J/kg)
τ	torque (N m)
ϕ	crank angle (deg)
ω	angular velocity (rad/s)

Subscripts

o	initial/atmospheric conditions
c	coolant
e	engine
f	fuel
g	gas
in/ex	inlet/exhaust
L	load or loss
w	wall or work

Abbreviations

°CA	degrees crank angle
bmep	brake mean effective pressure (bar)
fmep	friction mean effective pressure (bar)
isfc	indicated specific fuel consumption (g/kW h)
LHR	low heat rejection
PSZ	plasma spray zirconia
rpm	revolutions per minute
SN	silicon nitride

termed irreversibility – is the source for the defective exploitation of fuel into useful mechanical work in an internal combustion engine [7,8]. The reduction of irreversibilities can lead to better engine performance through a more efficient exploitation of fuel.

Moreover, during the last three decades an increasing interest in the low heat rejection (LHR) diesel engine is noticed. The objective of a low heat rejection cylinder is to minimize heat loss to the walls, eliminating the need for a coolant system. This is achieved through the increased level of temperatures inside the cylinder resulting from the insulation applied to the cylinder walls. By so doing, a reduction can be observed in ignition delay (thus combustion noise), hydrocarbons and particulate matter emissions, and also an increase in engine performance and additional exhaust energy. A major issue here is the decrease in the volumetric efficiency, hence power output, and the increase in NO_x emissions.

As regards steady-state operation, various researchers have studied the LHR engine by applying either first- (e.g. [9–12]) or second-law (e.g. [13–17]) balances. Only a few works, however, have treated this subject during the very important transient operation with the results limited to the (first-law) engine speed response [1,18,19]. The main finding was that a higher wall temperature slightly improved the turbocharger lag and thus speed response.

It seems therefore logical to expand on the investigation of cylinder wall insulation for both energy and exergy balances of a turbocharged diesel engine when operating under transient load conditions. In a previous publication by the present author [20], the effect of cylinder wall temperature variation on the second-law transient response had been investigated on a somewhat theoretical basis. In this paper a more detailed analysis will be carried out on a practical basis, with the depth of insulation being now the external variable. Special attention will be paid to the comparison between the two thermodynamic laws results.

The computer code developed follows the filling and emptying approach and incorporates some important features to account for the peculiarities of transient operation. Improved relations/sub-models have been developed concerning fuel pump operation, dynamic analysis and friction during transients, whereas each cylinder of the multi-cylinder engine is treated individually and sequentially.

Two insulators, common in current engineering practice, for the engine in hand are studied, i.e. silicon nitride (SN) and plasma spray zirconia (PSZ); their results are compared to the nominal non-insulated operation.

The analysis carried out will be given in a series of multiple diagrams, which depict the interesting first- and second-law values with special reference to the various irreversibilities. Owing to the narrow speed range of the engine in hand, only load increases under constant governor setting are investigated, which, nonetheless, play a significant role in the European transient cycles of heavy duty vehicles.

2. Background on second-law analysis of steady-state, low heat rejection, diesel engine operation

The analysis of Alkidas [13] showed that a higher temperature of the reactants (i.e. through insulation of the cylinder walls) increases the flame temperature and

significantly decreases the combustion irreversibilities. At the same time the wall insulation increases the amount of the availability term of the exhaust gas from cylinder. The above results were confirmed by Caton [14]. Rakopoulos et al. [17] concluded that the interest for LHR engines emanates from their potential to do more work by utilizing the exhaust gases in a Rankine bottoming cycle or a power turbine.

A higher insulation significantly limits the availability destruction associated with heat transfer from the gas to the cylinder walls [15,16]. This availability potential can then be extracted with the use of heat transfer devices driving secondary energy extraction units. It is imperative that the engine working fluid should not be used for such devices, since its low temperature level would make a very poor work recovery, i.e. with the heat transfer from the cylinder walls to the cooling water the majority of the work potential is destroyed.

The second-law efficiency is also expected to increase with insulation. This is mainly attributed to the reduced percentage heat losses and the resulting increase in flame temperature [13].

3. First-law analysis

3.1. Simulation process

Since the present analysis does not, at the moment, include prediction of exhaust emissions and on the other hand deals with transient operation calculations on a °CA basis, a single-zone model is used for the evaluation of thermodynamic processes [1–4].

For heat release rate predictions, the fundamental model proposed by Whitehouse and Way [21] is used. Especially during transients, the constant K in the (dominant) preparation rate equation of the Whitehouse–Way model is correlated with the Sauter mean diameter (SMD) of the fuel droplets through a formula of the type $K \propto (1/\mathrm{SMD})^{2.5}$ [21].

The improved model of Annand and Ma [22] is used to simulate heat loss Q_L to the cylinder walls,

$$\frac{dQ_L}{dt} = F\left\{\frac{k_g}{D}Re^b\left[a(T_g - T_w) + \frac{a'}{\omega}\frac{dT_g}{dt}\right] + c\left(T_g^4 - T_w^4\right)\right\} \quad (1)$$

where a, a', b and c are constants evaluated after experimental matching at steady-state conditions, $F = 2(\pi D^2/4) + F'$, with $F' = \pi D x$, and x the instantaneous cylinder height in contact with the gas [3,21], k_g is the gas thermal conductivity, and the Reynolds number Re is calculated with a characteristic speed derived from a k–ε turbulence model and a characteristic length equal to the piston diameter.

During transient operation, the thermal inertia of the cylinder wall is taken into account using a detailed heat transfer scheme. This is depicted in Fig. 1. It holds

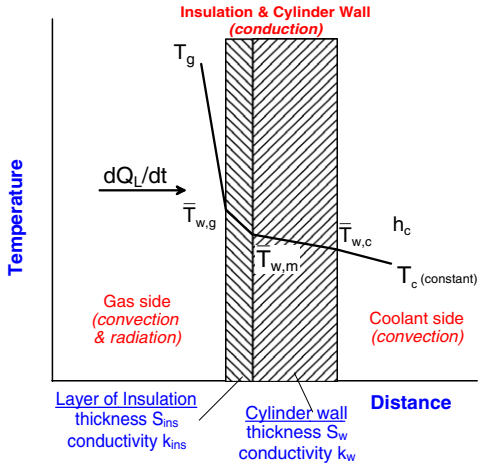

Fig. 1. Heat convection–conduction scheme for engine cylinder.

$$\frac{1}{4\pi}\int_0^{4\pi}\frac{1}{F'}\frac{dQ_L}{d\varphi}\,d\varphi = \frac{k_{ins}}{S_{ins}}(\overline{T}_{w,g} - \overline{T}_{w,m}) = \frac{k_w}{S_w}(\overline{T}_{w,m} - \overline{T}_{w,c}) = h_c(\overline{T}_{w,c} - T_c) \quad (2)$$

where $dQ_L/d\phi$ is the heat flux computed from Eq. (1), bearing also in mind that $d\phi = 6N\,dt$, S_{ins} the thickness of the insulation layer with k_{ins} its thermal conductivity, S_w the cylinder wall thickness with k_w its thermal conductivity, h_c the heat transfer coefficient from the external wall side (respective temperature $\overline{T}_{w,c}$) to the coolant; the overbar denotes mean temperatures over an engine cycle. Eq. (2) is solved for the three unknown variables, i.e. the wall temperatures $\overline{T}_{w,g}$, $\overline{T}_{w,m}$ and $\overline{T}_{w,c}$, which change from cycle to cycle during the transient event but are considered to remain constant throughout the cycle.

Various sophisticated sub-models have been incorporated in the main code, which have been analysed in previous publications [3,4,23]. These deal with:

Multi-cylinder engine modelling: At steady-state operation the performance of each cylinder is essentially the same, due to the quasi-steady position of the governor clutch resulting in the same amount of fuel being injected per cycle, and the quasi-steady turbocharger compressor operating point. Under transient operation, however, each cylinder experiences *different* fuelings and air mass flowrates during the same engine cycle. This occurs due to the combined effect of: (a) the continuous movement of the fuel pump rack that is initiated by a load or speed change and (b) the continuous movement of the turbocharger compressor operating point. As regards speed changes, only the first cycles are practically affected. However, when load changes are investigated, significant variations can be experienced throughout the whole transient cycle. The usual approach, here, is the solution of the governing equations for one cylinder and the subsequent use of suitable phasing images of this cylinder's behavior. This approach is widely popular for limiting the computational time [1]. Unlike this, a true multi-cylinder engine model has been

developed. Here, all the governing differential and algebraic equations are solved individually for every one cylinder of the six-cylinder engine under study according to the current values of the fuel pump rack position and turbocharger compressor flow. This results in (significant) differentiations in both fueling and air mass flow-rates for each cylinder during the *same* cycle of a transient event. The current approach has, of course, the drawback of increasing the computational time almost linearly to the number of cylinders involved.

Fuel pump operation: Instead of using steady-state fuel pump curves during transients, a fuel injection model, experimentally validated at steady-state conditions, is applied. Thus, simulation of the fuel pump-injector lift mechanism is accomplished, taking into account the delivery valve and injector needle motion. The unsteady gas flow equations are solved using the method of characteristics, providing the dynamic injection timing as well as the duration and the rate of injection for each cylinder at each transient cycle. The obvious advantage here is that the *transient* operation of the fuel pump is also taken into account. This is mainly accomplished through the fuel pump residual pressure value, which is built up together with the other variables during the transient event.

Friction: For the calculation of friction inside the cylinder, the model proposed by Taraza et al. [24] is adopted; it describes the non-steady profile of friction torque during each cycle based on fundamental friction analysis. Here, the total amount of friction is divided into four parts, i.e. piston rings assembly, loaded bearings, valve train and auxiliaries. Total friction torque at each °CA is the sum of the above terms; it varies during the engine cycle, especially around 'hot' TDC, unlike the usually applied 'mean' fmep equations where friction torque remains constant throughout each cycle [4,23].

The *conservation of angular momentum* applied to the engine crankshaft yields

$$\tau_e(\varphi,\omega) - \tau_{fr}(\varphi,\omega)_{trans} - \tau_{Load}(\omega) = G_{tot}\frac{d\omega}{dt} \tag{3a}$$

where G_{tot} is the engine-flywheel-load mass moment of inertia and $\tau_e(\phi,\omega)$ stands for the instantaneous value of the engine torque [4]. Also,

$$\tau_{Load}(\omega) = c\omega^2 \tag{3b}$$

is the load torque for the hydraulic brake coupled to the engine examined, and $\tau_{fr}(\phi,\omega)_{trans}$ stands for the friction torque.

3.2. Experimental procedure

The objective of the experimental test bed developed was to validate the transient performance of the engine simulation. To accomplish this task the engine was coupled to a hydraulic brake (dynamometer). The experimental investigation was conducted on a (un-insulated) MWM TbRHS 518S, six-cylinder, turbocharged and aftercooled, medium-high speed diesel engine. The engine is permanently coupled to a Schenck hydraulic dynamometer. Details about the experimental setup can be found in Ref. [3]. The basic data for the engine and turbocharger are given in Table 1.

Table 1
Engine data

Engine Type	Six-cylinder, 4-stroke, turbocharged and aftercooled, heavy-duty, water-cooled diesel engine
Speed range	1000–1500 rpm
Bore/stroke	140 mm/180 mm
Maximum power	236 kW @ 1500 rpm
Maximum torque	1520 Nm @ 1250 rpm
Moment of inertia (engine and load)	15.60 kg m^2

The first requirement from the engine test bed instrumentation was to investigate the steady-state performance of the examined engine. For this purpose, an extended series of steady-state trials was conducted in order on the one hand to examine the model's predictive capabilities and on the other to calibrate successfully the individual sub-models. The investigation of transient operation was the next task. Since the particular engine is one with a relatively small speed range, mainly load changes (increases) with constant governor setting were examined. A typical example of a conducted transient experiment is given in Fig. 2. Here, the initial load was 10% of the full engine load at

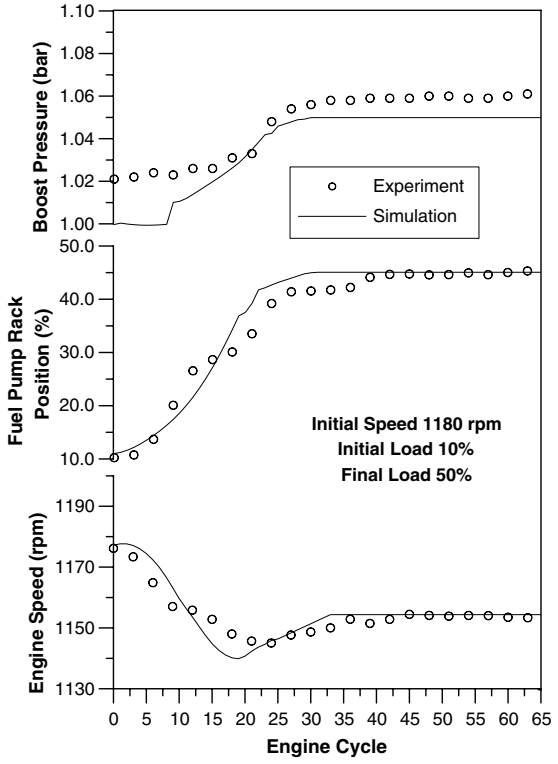

Fig. 2. Experimental and predicted engine transient response to an increase in load.

1180 rpm. The final load applied was almost 50% of the full engine load. The matching between experimental and predicted transient responses was satisfactory for both engine and turbocharger variables (engine speed, fuel pump rack position and boost pressure). We observe that the boost pressure is notably delayed compared to the speed profile owing to the well known turbocharger lag effect.

4. Second-law analysis

The availability balance equations are applied to the turbocharged diesel engine and all its subsystems, on a °CA basis [7,20,25,26]. For the jth engine cylinder it holds,

$$\frac{dA_j}{d\varphi} = \frac{\dot{m}^j_{in} b_{in} - \dot{m}^j_{ex} b_{ex}}{6N} - \frac{dA_w}{d\varphi} - \frac{dA_L}{d\varphi} + \frac{dA_f}{d\varphi} - \frac{dI}{d\varphi} \quad (4)$$

with $\dot{m}^j_{in}$ the incoming mass flow rate from the inlet manifold and $\dot{m}^j_{ex}$ the outgoing one to the exhaust manifold according to the first-law analysis of the multi-cylinder engine;

$$\frac{dA_w}{d\varphi} = (p_g - p_o)\frac{dV}{d\varphi} \quad (5)$$

is the availability term for the work transfer with p_g the instantaneous cylinder pressure,

$$\frac{dA_L}{d\varphi} = \frac{dQ_L}{d\varphi}\left(1 - \frac{T_o}{T_g}\right) \quad (6)$$

is the availability term for the heat transfer to the cylinder walls with T_g the instantaneous (uniform) cylinder gas temperature and $dA_f/d\varphi$ is the availability term for the injected fuel [6,7]. The term

$$b = h - T_o s - \sum_i x_i \mu^o_i \quad (7)$$

corresponds to the flow availability of the cylinder gas with x_i the mass fraction of species i in the mixture and μ^o_i the chemical potential of species i at the restricted dead state (i.e. when there exists thermal and mechanical equilibrium with the environment) [6,7]. The term $dI/d\phi$ in Eq. (4) represents the rate of irreversibility production within the cylinder. This consists mainly of the combustion term, while inlet-valve throttling and mixing of the incoming air with the cylinder residuals have a less than 5% contribution [7,25]. Similar expressions were derived for the second-law balance of manifolds, turbocharger and aftercooler [7,25,26].

5. Insulation schemes and transient schedules

The baseline, non-insulated, case configuration is that corresponding to the engine in hand, possessing a cast iron wall thickness of 10 mm. Table 2 illustrates the four, widely different, insulation schemes considered for the present study. The main thermal properties of the cylinder wall materials and insulators (ceramics) used are given in Table 3.

Table 2
Summary of the insulation schemes

	Cylinder wall material	Insulation	Depth of insulation (mm)
1	Cast iron	–	–
2	Cast iron	SN	4.0
3	Cast iron	PSZ	1.0
4	Cast iron	PSZ	1.5
5	Aluminium	–	–

Table 3
Thermal properties for cylinder wall materials and insulators

	Conductivity 'k' (W/m K)	Thermal diffusivity 'α' (m^2/s)
Cast iron	54	14×10^{-6}
Aluminium	180	78×10^{-6}
SN	10	2.80×10^{-6}
PSZ	1.0	0.90×10^{-6}

One of the main effects of engine heat insulation is the significant rise of combustion chamber wall temperatures and thus the higher thermal loading of the engine. This loading is assumed to be withstood by the engine, without paying any attention in this study to the examination of the developed thermal stresses and component deformations. In any case, these wall temperatures are realistic in terms of existing materials.

When comparing the transient response of different engine configurations, it is imperative that the initial operating point is kept the same for all examined cases. For the present study, at the initial engine speed of 1180 rpm, the initial load always corresponded to the same value of constant 'c' in the load torque term (Eq. (3b)). The latter was 10% of the engine's maximum load. Afterwards, a 650% relative load-change was abruptly applied. The final conditions roughly correspond to 75% engine load. The case with a 10–95% load-change will also be depicted in order to enhance the importance of some of the obtained results.

6. Results and discussion

Fig. 3 illustrates the corresponding mean, gas-side cylinder wall temperature $\overline{T}_{w,g}$ for each insulation scheme studied. Consistent with engineering intuition, a higher degree of insulation increases the wall temperatures throughout the transient event, as is also the case at steady-state operation [9,10]; this effect is enhanced with higher loading.

In Fig. 4, the response of four important engine values is illustrated, i.e. engine speed, fuel pump rack position, boost pressure and volumetric efficiency. Clearly, the engine speed, as well as the other variables of the engine and turbocharger, are only slightly affected by the level of temperatures inside the cylinder, with the higher insulated cases leading to smaller speed drops. This was also the result reached by Watson [1] and Schorn et al. [19] (the latter for acceleration transients), although these researchers did not investigate the effect of such a high level of insulation during transients. A higher wall temperature is

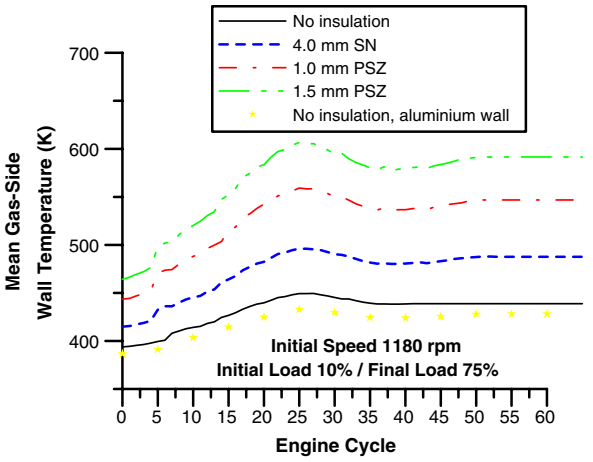

Fig. 3. Response of mean gas-side wall temperatures during the transient event (unless otherwise noted, the cylinder wall is cast iron).

generally expected to improve the turbocharger lag and thus speed response [4]. This is not so pronounced for the present engine, however, since its high total mass moment of inertia slows down the whole transient event. On the other hand, the volumetric efficiency shows a decreasing trend with higher insulation schemes, confirming the results of all the previous researchers during steady-state operation. Namely, the increased level of cylinder wall temperatures during the induction process transfers heat to the incoming charge, thus, reducing its density and, hence, volumetric efficiency throughout the transient event.

Fig. 5 expands the results of Fig. 4 by showing the response of the transient indicated specific fuel consumption (isfc) of the engine, highlighting the non-negligible benefit gained from the insulation. An increased level of temperatures during each cycle leads to 'fuller' pressures diagrams, thus increasing the efficiency up to 3.65% for the 1.5 mm PSZ case at the 20th cycle of the transient event. It is obvious that the engine handles now the transient test in a slightly more efficient manner. The difference between aluminium and cast iron non-insulated walls is modest, proving the very small effect of the cylinder wall material on the cycle transient efficiency. As the right sub-diagram shows, the response of the bmep is imperceptibly affected by the degree of insulation, with the highly insulated cases proving slightly more favourable. Here, the results are less distinguished than the isfc ones. This is mainly due to the decrease in the volumetric efficiency shown in the previous figure.

Fig. 6 focuses on the second-law balance and illustrates the evolution of four engine availability values during the transient event, i.e. work, heat loss to the walls, exhaust gas to ambient, and combustion irreversibilities; all are reduced to the fuel chemical availability. An increasing wall temperature results in increased charge temperatures and consequently lowers the degradation of the fuel availability since this is now transferred to 'hotter' gases. Thus, the combustion irreversibilities decrease throughout the transient test. For example, for the 1.5 mm PSZ case, the combustion irreversibilities decrease up to 23% compared to the non-insulated configuration.

It should be pointed out here that the combustion irreversibilities during transients evolve in a different way compared to the respective steady-state operation (i.e. for the same engine speed and fuel pump rack position). The difference is attributed to [27]:

- the differentiated fuel–air equivalence ratios experienced during transients owing to the turbocharger lag, which significantly affects the air–mass flow rate;

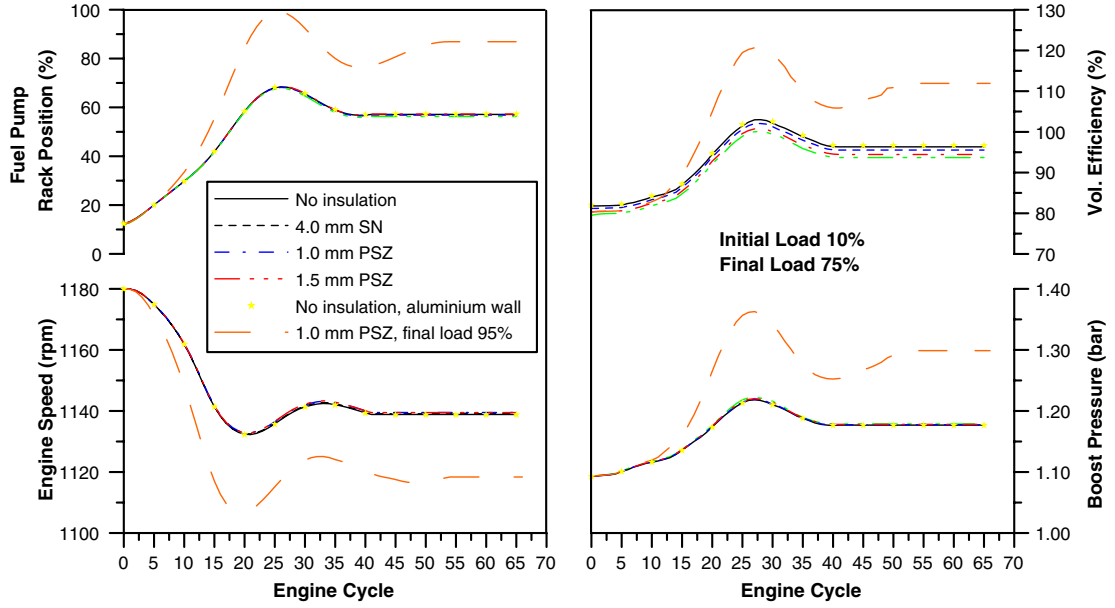

Fig. 4. Response of various engine parameters to an increase in load (unless otherwise noted, the cylinder wall is cast iron and the load increase is 10–75%).

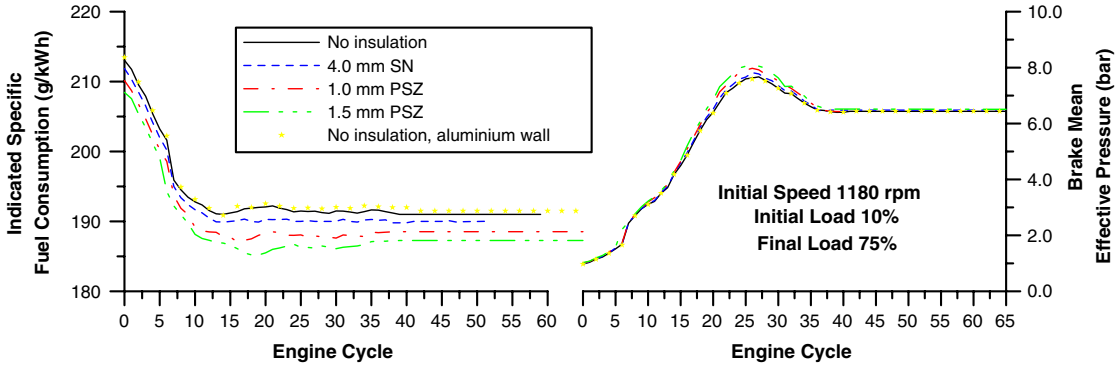

Fig. 5. Response of indicated specific fuel consumption and brake mean effective pressure to an increase in load (unless otherwise noted, the cylinder wall is cast iron).

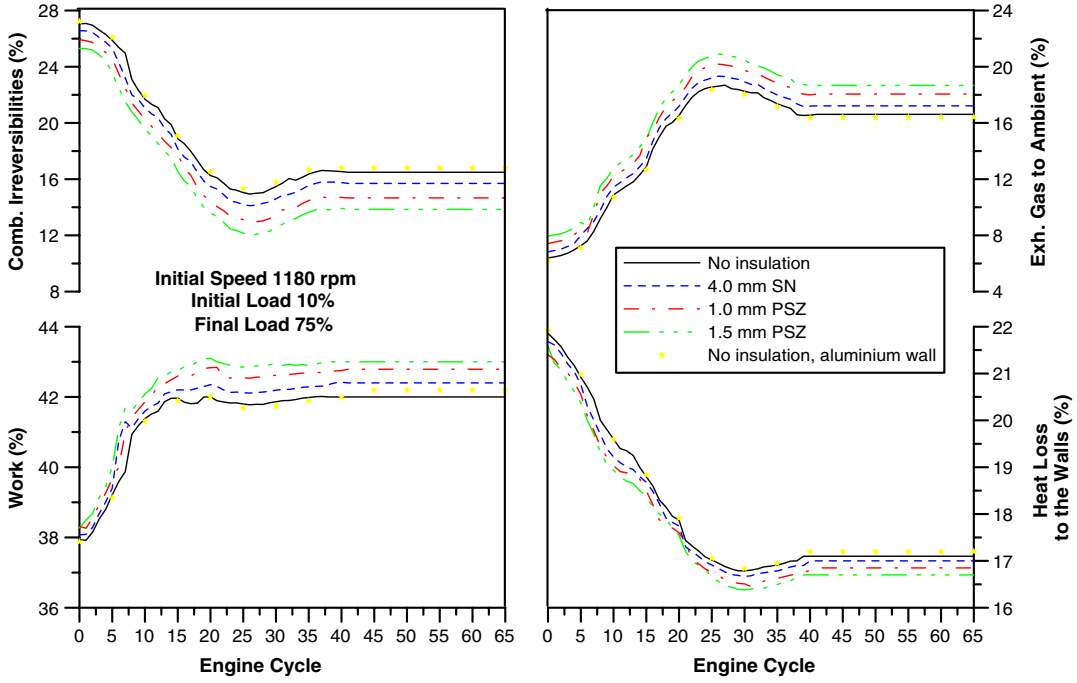

Fig. 6. Response of various second-law values to an increase in load (unless otherwise noted, the cylinder wall is cast iron).

- the transient operation of the fuel pump that differentiates from the steady-state fuel pump curves; and
- the fact that, during transients, integration of the left hand side of Eq. (4) over an engine cycle does not sum up to zero, as the initial conditions of the new cycle differ from the initial conditions of the previous one.

Unfortunately, although the combustion proceeded in a more efficient way, this was not transformed into increased piston work. Hence, the work term is only marginally improved (+2.3% at cycle no. 25 of the 1.5 mm PSZ case). This finding goes along with the bmep results depicted in Fig. 5, and with the conclusions reached by previous researchers during steady-state operation [17]. The reduction in combustion irreversibilities is reflected into an increase in the exhaust gas to ambient exergy. Both the absolute (in 'Joules') and percentage values of this term increased with higher insulation owing to the higher temperature of the working medium (see also Table 4). This availability amount can be afterwards recovered only if a bottoming cycle is applied.

On the other hand, a higher degree of insulation slightly decreases the exergy of heat loss to the cylinder walls when this is reduced to the fuel chemical availability. Eq. (6) shows that an increasing gas temperature T_g (depicted in Fig. 7) increases the 'quality' and, thus, the heat transfer availability from the cylinder gas (with reference to the ideal Carnot cycle, the engine thermal efficiency increases with higher temperature of the working medium). This is contradicted by the fact that a higher insulation scheme reduces the heat flux $dQ_L/d\phi$ to the cylinder walls. The combined effect of the above factors determines the trend for the percentage exergy term of heat loss depicted in Fig. 6. However, it should be highlighted that this exergy

Table 4
Maximum increase (at a particular cycle) in second-law values for the engine with 1.5 mm PSZ coating compared to the non-insulated operation

Work	+2.3%
Combustion irreversibilities	−23%
Total irreversibilities	−19%
Heat loss to the walls	−1.5%
Exhaust gas to ambient	+15%

term of heat loss to the walls possesses now a higher work potential, as the wall temperature has increased with insulation. A heat recovery device is needed in order for this availability to be exploited. At the moment, the subsequent heat transfer to the cooling medium practically causes its elimination.

Fig. 8 illustrates the response of the percentage irreversibilities during the transient event. The higher the degree of insulation, the lower the percentage of combustion irreversibilities. This trend is enhanced with higher loading. At the same time, other irreversibility terms such as exhaust manifold or turbine ones were found to increase since these depend on the condition of the exhaust gas.

This rather conflicting behavior can be explained if one looks deeper into the respective irreversibility production mechanisms. For the combustion term, the main mechanism comprises heat transfer from the burning of fuel to the gases. Consequently, the higher the temperature of the receiving gas (as is the case with increasing insulation) the lower the degradation of the fuel's chemical exergy, and hence the combustion irreversibilities. On the other hand, turbocharger aftercooler, inlet manifold and exhaust manifold irreversibilities are due to throttling, mixing and friction. These are, mainly, influenced by the level of pressures and temperatures of the working medium; thus, they increase with higher insulations.

The latter increase considerably with insulation as Figs. 3 and 7 suggest. Again, the case with aluminium wall only slightly distinguishes from the one with cast iron. In any case, it is important to note that the higher amount of exhaust manifold and turbine irreversibilities is always of much lesser importance throughout the whole transient

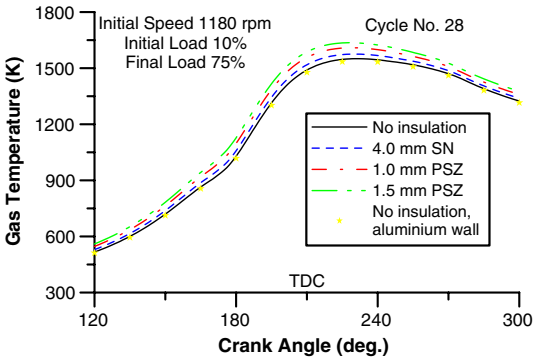

Fig. 7. Gas temperature variation during the 28th cycle of the transient event.

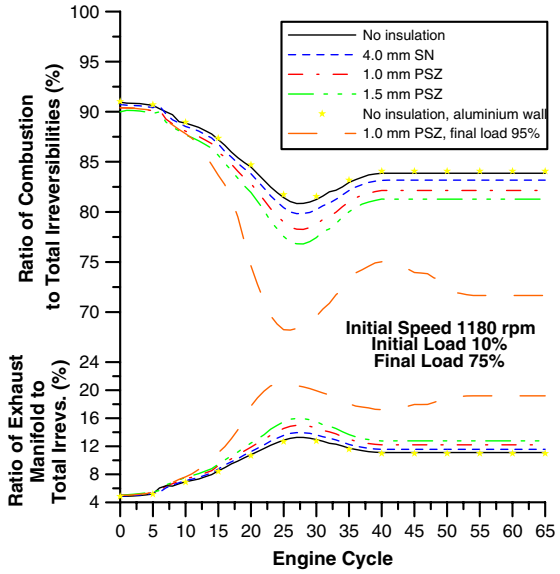

Fig. 8. Response of percentage combustion irreversibilities to an increase in load.

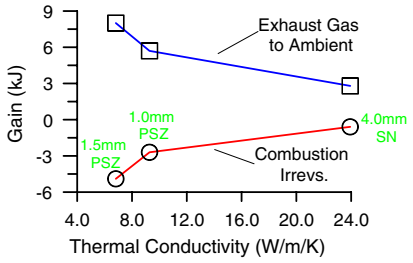

Fig. 9. Gain from insulation compared to the non-insulated operation for the whole transient event.

event. Even the absolute amount of the total engine irreversibilities (in 'Joules') decreases considerably (up to 19.5%) with higher insulation.

Finally, Fig. 9 quantifies the total gain from the insulation as regards two important second-law values, i.e. combustion irreversibilities (defined as 'theoretical' gain) and exhaust gas to ambient (defined as 'practical' gain), during the whole transient event. The gain in the work potential of the exhaust gas to ambient reaches 8 kJ or 2 kW during the 4 s of the transient event, for the 1.5 mm PSZ coating compared to the non-insulated operation and corresponds to a 2.4% increase in the engine brake power. This is the maximum extra power that can be obtained during the transient event from the increased insulation if we apply a bottoming cycle.

7. Summary and conclusions

An experimentally validated computer program was used to study the transient performance of a turbocharged diesel engine from the first- and second-law perspective, and for various insulation schemes:

- The transient response of the engine remains almost unaffected by the applied insulation. Certain steady-state findings, e.g. decrease in volumetric efficiency or isfc with higher insulation, were confirmed during transients too although the transient path differed from the respective steady state. On the other hand, the second-law values depend significantly on the applied insulation scheme.
- Combustion irreversibilities decrease considerably with higher insulation both in 'Joules' and as a percentage of either fuel availability (up to 23% at a certain cycle) or total irreversibilities.
- This decrease in the availability destruction was mainly transformed into an increase in the availability content of the exhaust gas to ambient (up to 2 kW for the 1.5 mm PSZ coating transient event). On the other hand, the respective heat loss availability remains practically unaltered.

The above results strengthen the belief that a combined optimisation based on both thermodynamic laws is required for better understanding and evaluation of internal combustion engines operation.

References

[1] Watson N. Dynamic turbocharged diesel engine simulator for electronic control system development. Trans ASME, J Dyn Syst Meas Control 1984;106(1/2):27–45.

[2] Winterbone DE. Transient performance. In: Horlock JH, Winterbone DE, editors. The thermodynamics and gas dynamics of internal combustion engines, vol. II. Oxford: Clarendon Press; 1986. p. 1148–212.

[3] Rakopoulos CD, Giakoumis EG, Hountalas DT, Rakopoulos DC. The effect of various dynamic, thermodynamic and design parameters on the performance of a turbocharged diesel engine operating under transient load conditions. SAE Paper No. 2004-01-0926; 2004.

[4] Rakopoulos CD, Giakoumis EG. Review of thermodynamic diesel engine simulations under transient operating conditions. SAE Paper No. 2006-01-0884; 2006.

[5] Obert EF, Gaggioli RA. Thermodynamics. New York: McGraw-Hill; 1963.

[6] Moran MJ. Availability analysis: a guide to efficient energy use. New Jersey: Prentice Hall; 1982.

[7] Rakopoulos CD, Giakoumis EG. Second-law analyses applied to internal combustion engines operation. Prog Energy Combust Sci 2006;32:2–47.

[8] Kyritsis DC, Rakopoulos CD. Parametric study of the availability balance in an internal combustion engine cylinder. SAE Paper No. 2001-01-1263; 2001.

[9] Assanis DN, Heywood JB. Development and use of a computer simulation of the turbo-compounded diesel engine performance and component heat transfer studies. SAE Paper No. 860329; 1986.

[10] Borman G, Nishiwaki K. Internal-combustion engine heat transfer. Prog Energy Combust Sci 1987;13:1–46.

[11] Alkidas AC. Performance and emission achievements with an uncooled heavy-duty, single-cylinder diesel engine. SAE Paper No. 890144; 1989.

[12] Rakopoulos CD, Mavropoulos GC. Modelling the transient heat transfer in the ceramic combustion chamber walls of a low heat rejection diesel engine. Int J Vehicle Des 1999;22:195–215.

[13] Alkidas AC. The application of availability and energy balances to a diesel engine. Trans ASME, J Eng Gas Turb Power 1988;110:462–9.

[14] Caton JA. On the destruction of availability (exergy) due to combustion processes – with specific application to internal-combustion engines. Energy 2000;25:1097–117.

[15] Flynn PF, Hoag KL, Kamel MM, Primus RJ. A new perspective on diesel engine evaluation based on second law analysis. SAE Paper No. 840032; 1984.

[16] Primus RJ, Hoag KL, Flynn PF, Brands MC. An appraisal of advanced engine concepts using second law analysis techniques. SAE Paper No. 841287; 1984.

[17] Rakopoulos CD, Andritsakis EC, Kyritsis DC. Availability accumulation and destruction in a DI diesel engine with special reference to the limited cooled case. Heat Recov Syst CHP 1993;13:261–76.

[18] Keribar R, Morel T. Thermal shock calculations in I.C. engines. SAE Paper No. 870162; 1987.

[19] Schorn N., Pischinger F, Schulte H. Computer simulation of turbocharged diesel engines under transient conditions. SAE Paper No. 870723; 1987.

[20] Rakopoulos CD, Giakoumis EG. The influence of cylinder wall temperature profile on the second-law diesel engine transient response. Appl Therm Eng 2005;25:1779–95.

[21] Benson RS, Whitehouse ND. Internal combustion engines. Oxford: Pergamon Press; 1979.

[22] Annand WJD, Ma TH. Instantaneous heat transfer rates to the cylinder head surface of a small compression-ignition engine. Proc Inst Mech Engrs 1970–1971;185:976–87.

[23] Rakopoulos CD, Giakoumis EG. Sensitivity analysis of transient diesel engine simulation. Proc Inst Mech Engrs – Part D: J Aut Eng 2006;220:89–101.

[24] Taraza D, Henein N, Bryzik W. Friction losses in multi-cylinder diesel engines. SAE Paper No. 2000-01-0921; 2000.

[25] Rakopoulos CD, Giakoumis EG. Availability analysis of a turbocharged diesel engine operating under transient load conditions. Energy 2004;29:1085–104.

[26] Rakopoulos CD, Giakoumis EG. Parametric study of transient turbocharged diesel engine operation from the second-law perspective. SAE Paper No. 2004-01-1679; 2004.

[27] Giakoumis EG, Andritsakis EC. Irreversibility production during transient operation of a turbocharged diesel engine. Int J Vehicle Des 2007;45(1/2):128–49.